AIAA-95-1722

An Efficient Means of Adaptive Refinement Within Systems of Overset Grids

Robert L. Meakin
Overset Methods, Inc.
at NASA Ames Research Center
Moffett Field, CA 94035-1000

12th AIAA Computational Fluid Dynamics Conference
June 19-22, 1995 / San Diego, CA

An Efficient Means of Adaptive Refinement Within Systems of Overset Grids

Robert L. Meakin†
Overset Methods, Inc.
at NASA Ames Research Center M/S 258-1
Moffett Field, CA 94035

Abstract

An efficient means of adaptive refinement within systems of overset grids is presented. Problem domains are segregated into near-body and off-body fields. Near-body fields are discretized via overlapping body-fitted grids that extend only a short distance from body surfaces. Off-body fields are discretized via systems of overlapping uniform Cartesian grids of varying levels of refinement. A novel off-body grid generation and management scheme provides the mechanism for carrying out adaptive refinement of off-body flow dynamics and solid body motion. The scheme allows for very efficient use of memory resources, and flow solvers and domain connectivity routines that can exploit the structure inherent to uniform Cartesian grids.

INTRODUCTION

The need for accurate predictive ability of the aerodynamics about geometrically complex bodies in steady and unsteady environments is obvious. Experimental investigative techniques, of course, continue to be invaluable. However, there are many problems of practical importance that are not amenable to experimental investigation without ignoring dynamic effects, or invoking other simplifications. For example, aircraft launch vehicle staging, conventional fixed-wing and rotary-wing aircraft store separation, and pilot ejection are examples of applications which cannot be fully studied experimentally due to several practical constraints. Mature computational methods such as empirically-modified, three-dimensional panel codes and nonlinear potential methods with ad hoc models are in common use. However, these methods cannot be relied upon for applications which may violate their inherent limitations. Vortical wakes, viscous effects, moving shocks, and aerodynamic interference between moving and stationary body components are particularly important for many applications. These problems demand the most advanced unsteady, three-dimensional Navier-Stokes solvers available. The fact that such problems can be studied computationally using integrated Navier-Stokes solvers and body-dynamics routines has been demonstrated previously.[1-4] However, the physical complexity of such problems, such as the motion of flow structures and/or body components, often makes it difficult to provide grid points in sufficient densities to ensure solution accuracy.[5]

The methods presented in this paper have been motivated by the need for adaptive refinement capability to maintain solution accuracy for geometrically complex problems, and by a desire to exploit the many advantages offered by an approach that uses overlapping systems of structured grids. The method of adaptive refinement presented in the following pages divides the physical domain for a given problem into "near-body" and "off-body" regions. The near-body portion of a domain is defined to include the surface geometry of all bodies being considered and the volume of space extending a short distance away from the respective surfaces. The construction of near-body grids and associated intergrid connectivity is a classical Chimera-style[6] decomposition of the near-body domain. In the present case, it is assumed that near-body grids provide grid point distributions of sufficient density to accurately resolve the flow physics of interest (i.e., boundary-layers, vortices, etc.) without the need for refinement. This is a reasonable constraint since near-body grids are only required to extend a short distance away from body surfaces. However, in the future, if the need exists, a method of adaptive refinement within near-body grids will also be developed.

The present method of adaptive refinement is designed to provide resolution of off-body dynamics associated with complex flow features and/or the motion of body components. The off-body portion of the domain is defined to encompass the near-body domain and extend out to the far-field boundaries of the problem. The off-body domain is filled with overlapping uniform Cartesian grids of variable levels of refinement. All adaptive refinement takes place within the off-body component grids. Initially, regions of the off-body field are marked for

†*Staff Scientist, Member AIAA*

grid systems. A simple example involving an airfoil and background Cartesian grid is given in Figure 1. Any point that lies within the body of a neighboring grid system is not a valid field point. Accordingly, such points are "blanked out" (see references[9,10]), and do not influence the solution. The hole boundary points in the background grid caused by the airfoil, and the airfoil outer boundary points are indicated in Figure 1. In an overset grid approach, definition of flow variables on such intergrid boundary points is accomplished by interpolation from solutions in the overlap region of neighboring grid systems. Generalized algorithms for carrying out this task automatically have been developed.[9-14]

In the methods presented in this paper, the near-body (body-fitted) grids are of classical Chimera construction. That is, bodies which are overset on portions of neighboring grid components cause holes, and intergrid boundary conditions must be provided for the resulting intergrid boundaries. The only added constraint in the present case is that near-body grids must resolve all flow features of significance within their domain. The maximum spacing in the near-body grids should be representative of the highest level of refinement provided via adaption within the off-body grids. Accordingly, the present off-body method of adaption will preserve the fidelity and accuracy of all flow dynamics that emanate from near-body grid components.

Adaptive Refinement: Off-body Grid Generation

The primary difference between a classical Chimera approach and what is being presented here as a means of adaptive refinement relates to the way the background, or off-body field, is being treated. In the former case, the background grids are static. In the present method, the background grids are dynamic and provide the entire means of adaptive refinement.

The method of grid generation presented here is valid for static and dynamic cases. Consider a set of near-body grids in their initial static (mated) positions, or in their dynamic positions at the start of an adaption step. We seek a completely automatic and efficient means of grid generation to discretize the off-body field. As an example, consider the tiltrotor and wing configuration illustrated in Figure 2. Given a set of near-body grids, the desired distance from the near-body boundaries to the far-field outer boundary D_{far}, and an indication of the existence and location of planes of symmetry, it is possible to efficiently generate a high quality system of off-body grids. It is also useful if the near-body grid components can be associated, or grouped, into distinguishable bodies. For example, in the tiltrotor configuration shown

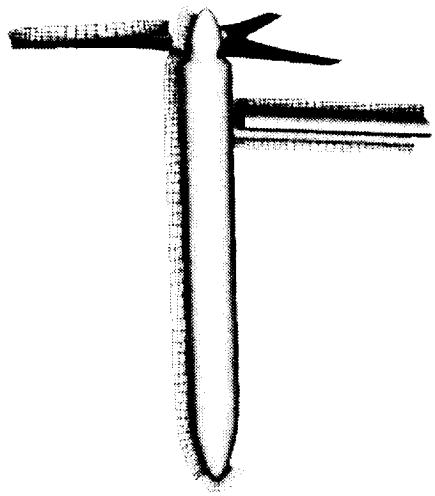

Figure 2. Tiltrotor configuration and selected surfaces of the near-body grid system.

in Figure 2, the initial distribution of grid-points in the off-body field can be done more efficiently if the near-body grid components associated with the flapped-wing are grouped into one body, those associated with the nacelle assembly with a second body, and those for the three rotor blades with a third body. Figure 3 shows midspan locations of all level-1 off-body grids that result for different groupings of the near-body component grids.

Parameters derived from the near-body grids

Geometric information contained in the near-body grid definitions furnish the present off-body grid generator with several important parameters. The grid spacing associated with the highest level of refinement S_{near} is set equal to the average maximum spacing detected in the near-body components. Of course, the near-body spacing could be ignored and S_{near} specified independently. If this is done, S_{near} should be set to a value that is less than or equal to the resolution available in the near-body grids. Otherwise, solution accuracy cannot be ensured via adaptive refinement. The near-body grids also furnish coordinates to bounding box diagonals which are used to construct the off-body grids. The diagonals that are needed include one for each body in the problem (r_{ij}^n), and one which bounds the off-body outer boundaries (R_{ij}). Here, the subscript i denotes the diagonal end-point (i = 1 is the left-front-bottom corner of the bounding box, and i = 2 is the right-back-top corner) and j denotes the three Cartesian coordinate directions. The superscript n denotes the body to which r_{ij}^n refers. For example, when three bodies are specified for the tiltrotor example indicated in Figure 3c, the near-

A_{max}). The spacings defined for each level of refinement form a vector, S_m. The m elements of S are ordered from fine to coarse, S_1 being equal to S_{near}. The iteration begins with an assumed amplification factor A, and an assumed number of refinement levels M. If the assumed values of A and M are used, the distance to the off-body outer boundary L can be computed as

$$L = \sum_{m=1}^{M} (\vartheta_{min} S_1 A^{(m-1)}) \tag{4}$$

If the computed value of L is less than $D_{far} - tol$, then the value of the spacing amplification factor A is increased. If the value of L is greater than $D_{far} + tol$, then A is decreased. The final value of A is arbitrarily limited between A_{min} and A_{max}. If the value of A drops below A_{min}, the advantage of increasing grid refinement from one level to the next is of marginal benefit. Conversely, if A grows to values larger than A_{max}, the grid spacing between successive levels of refinement become intolerably large. Accordingly, if A drops below A_{min} the number of refinement levels M is decreased by one, or, if A grows above A_{max}, M is increased by one.

Setting the state variable $\mathcal{B}$

Initialization of the state variable $\mathcal{B}$ is accomplished by checking the proximity of master-brick element centers to the near-body grids. For example, suppose we have associated N bodies with the tiltrotor configuration shown in Figure 2, and want to mark all master-brick elements of refinement level m. For each of the N bodies, coordinates of the body bounding boxes can be defined with an added border associated with the m^{th} level of refinement

$$\begin{aligned} x^n_{1j} &= r^n_{1j} - \{ \sum_{i=1}^{m} (\vartheta_{min} S_1 A^{(i-1)}) \} \\ x^n_{2j} &= r^n_{2j} + \{ \sum_{i=1}^{m} (\vartheta_{min} S_1 A^{(i-1)}) \} \end{aligned} \tag{5}$$

The values of x^n_{1j} and x^n_{2j} can be substituted into Equation (3) to determine the volume of computational space to visit in setting $\mathcal{B}$. For all points i_j visited in the master brick grid, $\mathcal{B}$ will be set to level m if the respective element center is within the bounding box and has not been previously set to a higher level of refinement. This procedure is repeated for all bodies N and each of the M levels of refinement.

During the flow simulation, error estimates are made and a list of points that have been flagged for refinement/coarsening is constructed. The coordinates of the points in this list are used to access the master-brick grid state variable using Equation (3) and to increment/decrement the value of $\mathcal{B}$ accordingly.

Coalescence of Bricks

The master-brick grid state variable $\mathcal{B}$ provides a very powerful tool for controlling off-body grid generation and adaptive refinement. $\mathcal{B}$ provides the benefits of structured data to an otherwise unstructured collection of refinement-wise heterogeneous bricks. In order take full advantage of the structure it is necessary to allow all master-brick elements of like level of refinement to coalesce into fewer bricks that occupy proportionately larger portions of contiguous computational space. The problem of coalescing neighboring bricks of like spacing does not have a unique solution. The final coalescence solution is sensitive to the sequence of coalescence. However, the issue of uniqueness is of little or no concern here. We simply want to deal with as few off-body grid components as necessary. Whether, or not, the absolute minimum number of bricks (which become off-body grid components) has been determined is not relevant. It is only necessary to reduce the number of bricks as much as is reasonably possible. Accordingly, in the present work, coalescence of bricks in $\mathcal{B}$ proceeds in sweeps of the three Cartesian coordinate directions X_j. In the future, it is anticipated that this approach will be implemented within parallel computing environments. Hence, the coalescence rules adopted here can easily be modified to produce the number and size of bricks subject to load balancing and system resource availability constraints.

A simple example of coalescence sweeps in the Cartesian coordinate directions is given in Figure 4. A plane of master-brick elements are shown in Figure 4a. Assume that the unshaded elements are bricks that have been assigned the same level of refinement. There are 174 such elements shown. Coalescence in the X_1 direction results in the bricks shown in Figure 4b (46 bricks). Then, taking the result of the X_1 coalescence sweep, bricks can be coalesced further in the X_2 direction to produce the 25 bricks shown in Figure 4c. The structure of the master-brick grid and state variable $\mathcal{B}$ allow coalescence to be carried out very efficiently.

Generation of off-body component grids

Once $\mathcal{B}$ has been used to coalesce bricks of like level of refinement, generation of the off-body component grids is trivial. Each off-body component grid is a uniform Cartesian distribution of points and can be completely defined using the diagonal that bounds the respective coalesced brick, and the brick refinement

level. In order to provide grid overlap, generation of the off-body component grids extend 1 grid interval outside every face of the coalesced brick. Figure 5 shows selected surfaces from off-body component grids generated for a) a wing/pylon/finned-store configuration and b) the tiltrotor configuration shown originally in Figure 2. The total computational expense required to generate these grids is minimal (i.e., several hundred thousand points/second on an SGI Indigo-2, R4400). Generation of each set of off-body grids is fully automatic and requires only the near-body grids, D_{far}, symmetry plane identification, and body grouping information.

Adaptive Refinement: Error Estimation

The ultimate success of an adaptive refinement scheme in maintaining solution accuracy rests to a great degree on the algorithms ability to detect significant errors in computed solutions. The subject of error estimation has a large literature. However, the various schemes can generally be categorized into two classes: phenomenon detection and error estimation. In the former class, schemes are developed to detect important flow phenomenon (i.e., shocks, vortices, etc.) so that points can be added to improve resolution of the phenomenon. In the latter class, schemes are developed in an attempt to measure numerical error so that points can be added to reduce the error.

Phenomenon based error indicators tend to be problem sensitive. What works well for one flow phenomenon may not work well for others, or the phenomenon threshold-level that works well in one application may be inappropriate for another. On the other hand, schemes designed to estimate numerical error tend to be computationally more expensive and have been met with varying degrees of success.[15,16]

In the present method a scheme has been implemented to estimate the numerical error. This approach was adopted in the hopes of achieving more generality and robustness than would otherwise have been attainable. The error at any point in a given component grid is defined as

$$E_{est} = Q - \hat{Q} \tag{6}$$

where Q is the dependent variable vector obtained via solution of the equations of motion using an a^{th}-order flow solver. $\hat{Q}$ is the dependent variable vector obtained via interpolation from surrounding points in space using an a^{th} order interpolation scheme.

The formal accuracy of a numerical method is generally stated in terms of its Taylor error, E_t. Before proceeding further with the present discussion, a definition of numerical accuracy is given as a point of reference. A partial derivative of the form $\partial^b f/\partial x^b$ can be expressed as the sum of the difference approximation to be employed and E_t.

$$\frac{\partial^b f}{\partial x^b} = FDE + \Delta x^{(c-b)} \frac{\partial^c f}{\partial x^c} + \ldots \tag{7}$$

The "order" of the difference approximation is therefore $(c-b)$, where b is the order of the partial derivative being approximated, and c is the order of the leading partial derivative in E_t. The difference scheme is then said to be an a^{th} order scheme, where $a = c - b$. This definition holds for time, space, and mixed derivatives regardless of how step-sizes have been arranged in the expression of the scheme.

The flow solver that will be employed for testing the present adaptive refinement method is formally 2nd order in space and optionally 1st or 2nd order in time. For unsteady applications it is proposed that the time-step be chosen to be consistent with the near-body grids and provide good temporal resolution of all flow features being directly simulated. This being the case, spatial error is used here to drive the adaptive refinement process. In order to employ the error estimator given by Equation (6), a 2nd order interpolation scheme must be used to determine $\hat{Q}$. It is easy to show that tri-linear interpolation of the dependent flow variables is second order accurate in space ($b = 0$ and $c = 2$).

Even though Equation (6) provides a means to estimate the numerical error in the computed solution, alone it lacks criteria for error significance in terms of grid refinement and coarsening. According to Equation (7), the dimensionless error of a 2^{nd} order flow solver should be proportional to Δx^2. Therefore, the needed threshold criteria for error significance is defined here to be

$$E_{ref} \approx Q_\infty \Delta x^2 \tag{8}$$

$$E_{cor} \approx \frac{Q_\infty}{2A} \Delta x^2 \tag{9}$$

where Δx is set equal to S_{near}, Q_∞ is the free-stream dependent variable vector, and A is the grid refinement amplification factor. Hence, if the estimated error at any point in an off-body component grid is greater than a 2^{nd} order error in the near-body grids, the master-brick element associated with that point will be flagged for refinement. Conversely, if the maximum error of all points within a given master-brick element are at least

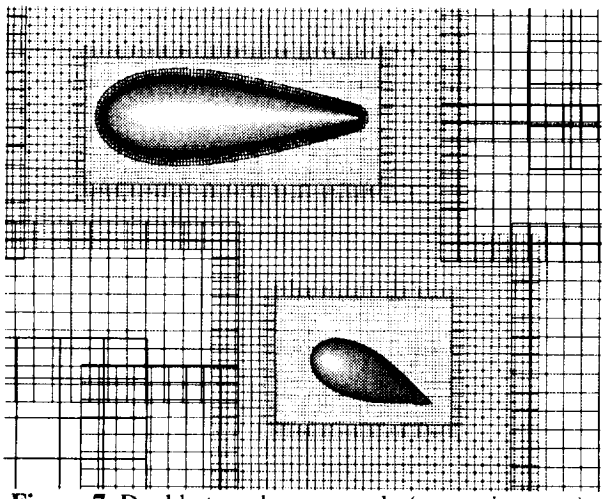

Figure 7. Double tear-drop example (separation case). Proximity based rules of adaption used alone to generate off-body grid components about near-body grid components subsequent to separation of small tear-drop.

cedure, but only combining them with the proximity based rules of adaption is not sufficient. Figure 8 illustrates the deficiency of an adaption procedure that ignores step 5 of Procedure 2. The illustration assumes static body conditions (steady, or unsteady flow) with adaption steps every "m" time-steps. Adaption is in response to a developing wake behind the tear-drop pair. The adaption sequence depicted in the figure shows that without memory of the previous refinement level settings, regions of off-body space can erroneously be refined and coarsened in alternate adaption steps.

Procedure 2, step 5 constitutes a "memory" of the master-brick grid state variable $\mathcal{B}$. Memory of $\mathcal{B}$ settings at the last adaption step combined with proximity rules and error estimate results remedies the defect illustrated in Figure 8. The general effect of step 5 is illustrated in Figure 9 where proximity rules and $\mathcal{B}$ settings memory (step 5) are used to adapt to the motion of the small tear-drop. Rather than providing high resolution around the separate near-body grid systems (as in Figures 6 and 7), a swath of high resolution grids are generated along the path traversed by the moving body. Off-body flow structures are often dragged, at least for some duration of time, along the path taken by bodies moving relative to other body components. This is true for the store separation-like problems suggested by the tear-drop example. Since high resolution off-body grids also automatically follow in the wake of moving bodies (due to step 5), the role of error estimation will often be to *decrease* resolution in the wake of moving bodies when it is no longer required.

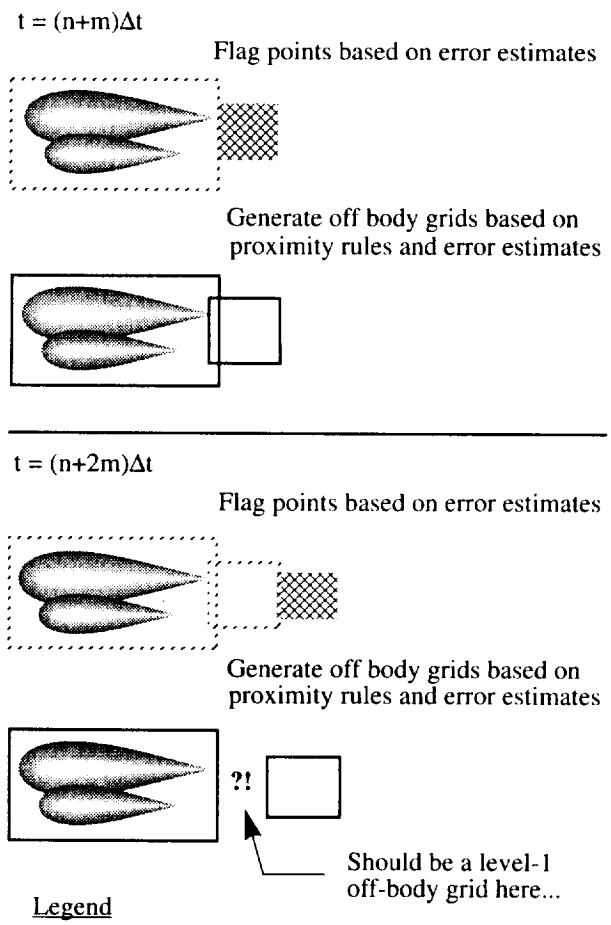

Figure 8. Error estimation and proximity rules alone are insufficient to govern general solution adaption method. The functionality of Procedure 2, step 5 is also needed.

Adaptive Refinement: Solution Transfer Between Pre- and Post-Adaption Off-Body Grids

During the course of an unsteady solution process, the off-body grid system will be required to adapt to the evolving flow dynamics and motion of body components. Of course, adaption will not be repeated at every time-step, but rather periodically. In any case, whenever it is necessary to repeat the adaption process, the problem of transferring an existing solution (pre-adaption step) onto a new off-body grid system will exist. Figure 10 is a simple illustration of the solution transfer problem.

In the figure, the light colored bricks represent values

A null response to the queries posed by Equation (10) indicate that grids "m" and "n" intersect. The range of grid "m" computational space that can be updated by grid "n's" solution can then be determined by relations similar to Equation (3), viz.

$$i_{1j}^{m} = int\left\{\frac{(x_{min} - X_{1j}^{m})}{\Delta X_{j}^{m}} + 1\right\}$$

$$i_{2j}^{m} = int\left\{\frac{(x_{max} - X_{1j}^{m})}{\Delta X_{j}^{m}} + 1\right\} \tag{11}$$

where

$$x_{min} = max\,(X_{1j}^{m}, X_{1j}^{n})$$

$$x_{max} = min\,(X_{2j}^{m}, X_{2j}^{n})$$

For the N pre-adaption step off-body grids

Bounding-box coordinates of grid n define volume of solution domain available for donation of solution data to new grid components

For the M new off-body component grids

1 test coordinates of grid m with those of grid n.

2 if volume m intersects volume n,

a) identify the grid m J,K,L space that is in common with grid n

b) find a donor element in grid n for each point in the J,K,L range identified for grid m

c) interpolate Q from grid n to grid m

Procedure 3. Procedure for solution transfer between pre- and post-adaption step off-body component grids.

Indices of the grid "n" element that bounds each point in the grid "m" computational space range defined by Equation (11) is easily determined from Equation (12). The expression that defines the relationship between Q at point i_j^m and the values of Q associated with element i_j^n is given as Equation (13). Definition of the l coefficients $[C(\xi_j)]_l$ depend on the particular interpolation scheme to be employed. Trilinear interpolation results in the definitions of $[C(\xi_j)]_l$ (where $l = 1, 2, \ldots, 8$) given in Equation (14).

$$i_j^n = int\left\{\frac{(x_j^m - X_{1j}^n)}{\Delta X_j^n} + 1\right\} \tag{12}$$

where $\quad x_j^m = (i_j^m - 1)\,\Delta X_j^m + X_{1j}^m$

$$Q^m = [C(\xi_j)]_l Q_l^n \tag{13}$$

where

$$\xi_j = (x_j^m - x_j^n)/\Delta X_j^n$$

$$x_j^m = (i_j^m - 1)\,\Delta X_j^m + X_{1j}^m$$

$$x_j^n = (i_j^n - 1)\,\Delta X_j^n + X_{1j}^n$$

$$\begin{aligned}
C_1 &= (1-\xi_1)\,(1-\xi_2)\,(1-\xi_3)\\
C_2 &= \xi_1\,(1-\xi_2)\,(1-\xi_3)\\
C_3 &= \xi_1\xi_2\,(1-\xi_3)\\
C_4 &= (1-\xi_1)\,\xi_2\,(1-\xi_3)\\
C_5 &= (1-\xi_1)\,(1-\xi_2)\,\xi_3\\
C_6 &= \xi_1\,(1-\xi_2)\,\xi_3\\
C_7 &= \xi_1\xi_2\xi_3\\
C_8 &= (1-\xi_1)\,\xi_2\xi_3
\end{aligned} \tag{14}$$

Interpolation of Q from element i_j^n to point i_j^m will be exact whenever $\xi_j = 0$ for $j = 1, 2, 3$. This situation can occur over entire grid components when grids "n" and "m" are at the same level of refinement.

Adaptive Refinement: Domain Connectivity

The final adaption-step listed in Procedure 1 corresponds to domain connectivity. In concept, the problem of establishing domain connectivity among the near-body/off-body overset grid discretizations suggested here is the same as for conventional Chimera style overset grids. However, in terms of data preparation and computational resource requirements, it is much more efficient to employ the present approach. The approach even ensures that optimal donor elements will always be

potential donors. Procedure 4, Step 3 indicates three classes. Class-1 includes all intergrid boundary points that originate from any near-body grid component (i.e., hole fringe and outer boundary points). Class-2 includes all intergrid boundary points that originate from level-1 off-body grid components (hole-fringe and outer boundary points). Both Class-1 and Class-2 intergrid boundary points have the potential for having near-body and off-body donors. Hence, the need for a distinction between these two classes is not obvious. During the course of a moving-body flow simulation, it is possible to use donor elements found for Class-1 intergrid boundary points at the previous time-step as a first guess for donor elements at the current time-step. The resulting computational advantage of such an approach can be significant. However, there is no correspondence in grid identification number for off-body grid components from one adaption step to the next. Therefore, a similar restart capability does not exist for Class-2 points, hence, the need for both classes. The third and final class identified in Procedure 4, Step 3 includes all intergrid boundary points that originate from level-2 and higher off-body grid components. Class-3 point donors can always be found in off-body grid components and, therefore, never require conventional search procedures.

Conventional donor search procedures are not discussed here, but are deferred to the literature.[9-14] The "fast" donor identification procedure noted in Procedure 4, Step 4 is trivial. If "m" denotes the off-body grid component identity of an intergrid boundary point, and "n" denotes the identity of the off-body grid component who's min/max box includes the intergrid boundary point in question, Equations (12-14) can be used directly to compute the corresponding donor element and interpolation coefficients. An algorithm based on Procedure 4 has been used to establish domain connectivity for the near-body/off-body discretizations of the tiltrotor geometry indicated in Figure 2, wing/pylon/finned-store geometry indicated in Figure 5, and double tear-drop geometry shown in Figure 6. Each case was carried out on an SGI Indigo-2 (R4400). Donor connectivity solutions were generated at an average rate of 2,950 IGBP/sec. These rates are comparable to those realizable on a Cray Y-MP/C-90 using the most efficient domain connectivity algorithm for conventional Chimera-type discretizations.[4]

SUMMARY

An efficient means of adaptive refinement within systems of overset grids has been presented. A novel off-body grid generation scheme has been developed that is very efficient and provides the mechanism for carrying out adaptive refinement of off-body flow dynamics and solid-body motion. The structure of off-body grids results in very efficient use of memory resources and facilitates the use of extremely efficient flow solvers and domain connectivity routines. Since, off-body grid generation is completely automatic, the method translates into substantial savings of human resources as well, even for static body and steady-state problems.

The primary elements of the algorithm, including error estimation, off-body grid generation, solution transfer between pre- and post-adaption step off-body grids, and domain connectivity have been developed and tested on a limited set of test problems. The algorithms still need to be integrated with a flow solver and tested on a range of applications to demonstrate performance and identify areas which need improvement.

ACKNOWLEDGEMENTS

This work was carried out under NASA ARC grant NCC2-747. The author wishes to acknowledge the influence of Dr. Kalpana Chawla for many insightful discussions on adaptive refinement. The idea for the off-body grid generator presented in this paper was born as a result of these discussions. Also, thanks is due to Professor Marsha Berger who provided needed encouragement with the idea to exploit the benefits of structured grids by providing adaptive refinement using structured blocks rather than unstructured cell subdivision methods.

REFERENCES

[1] Meakin, R. and Suhs, N., "Unsteady Aerodynamic Simulation of Multiple Bodies in Relative Motion," AIAA Paper 89-1996-CP, pp. 643-657, June 1989.

[2] Meakin, R., "Computations of the Unsteady Flow About a Generic Wing/Pylon/Finned-Store Configuration," AIAA Paper 92-4568-CP, pp. 564-580, August 1992.

[3] Lijewski, L. and Suhs, N., "Chimera-Eagle Store Separation," AIAA Paper 92-4569, August, 1992.

[4] Meakin, R., "Moving Body Overset Grid Methods for Complete Aircraft Tiltrotor Simulations," AIAA Paper 93-3350-CP, pp. 576-588, July 1993.

[5] Meakin, R., "On the Spatial and Temporal Accuracy of Overset Grid Methods for Moving Body Problems," AIAA Paper 94-1925-Cp, pp. 858-871, June 1994.

[6] Steger, J. L., Dougherty, F. C., and Benek, J. A., "A Chimera Grid Scheme," Advances in Grid Generation, K. N. Ghia and U. Ghia, eds., ASME FED-Vol